

# Response improvements in industrial DC drives derived from optimal analysis

B.J. Cardwell, B.Sc., Ph.D., A.M.I.E.E., and C.J. Goodman, M.A., Ph.D.,  
C.Eng., M.I.E.E.

*Indexing terms:* Computer applications, Optimal control

**Abstract:** A computer-based solution of the equations arising from the application of optimal control theory to a wide-speed-range DC drive reveals the manner in which the control should operate to achieve minimum error-squared performance. An examination of simulated conventional spillover schemes confirms that these are least able to approach the optimal performance in the spillover field-weakening control itself. An alternative field-weakening signal using a mix of speed reference, speed error and current signals is proposed which, simulation indicates, performs more closely to the optimised system in the upper speed ranges. Practical results from a laboratory implementation of this controller suggest that the modest performance improvement is achievable on industrial drives.

## 1 Introduction

This paper presents some results from the application of dynamic optimal control theory to typical industrial speed-controlled DC machine drives such as those used in rolling mills and process lines. Separately excited DC motors still hold a monopoly in these drives because of the relative ease with which they may be controlled.

In order to achieve a wide speed range, field weakening is necessary to take the speed above base speed. In the conventional controller this is done by means of a spillover field-weakening loop, where the armature voltage is monitored and used to reduce the field strength as the voltage approaches its rated value (typically over the range 95–100%). As this loop encompasses the relatively large field time constant and also experiences changing loop gain as the speed increases, it is a difficult problem to obtain a fast enough response in the spillover loop for the overall speed response to be adequate. In practical systems there is a tendency for voltage overshoot to occur in response to a step input; this is often prevented by imposing rate-of-change-of-speed reference limits.

Even if a straight-line magnetisation characteristic is assumed, the DC machine is still a strongly nonlinear device when under both armature and field control. The particular nonlinearities present are the multiplying terms found in the armature and torque equations. In order to derive a linear model it is necessary to assume constant field operation [1]. This step is justified to some extent as the field time constant is relatively much longer than the armature time constant; but the residual model is only second order and thus of limited use in modelling systems that utilise the full flexibility of the DC machine. Nevertheless, useful guidance can be obtained regarding basic design choices, such as performance index weightings, from studying the fixed-field model, and this is discussed in the next Section.

Numerical solution techniques can be employed to solve the two-point boundary value problem resulting from applying Pontryagin's maximum principle [2] to the nonlinear model including the multiplication terms. Results from the simple fixed-field linear model are used to provide sensible initial choices for weighting factors and boundary conditions. This technique is used here to estab-

lish optimal trajectories for machine responses under both field and armature voltage control, with armature current limiting, and for various performance criteria.

These optimal results are then used as a basis for comparison with a conventionally designed spillover field-weakening system. It is thus possible to distinguish the main characteristics of the optimal controller which enable it to achieve a slightly better performance. As is often the case, real-time solution of the optimal scheme as a feedback controller is impractical [3], but the form of the responses suggests a modification to the conventional control scheme which results in a nearer optimal performance.

## 2 Optimal analysis of DC machine controls

### 2.1 Frequency domain approach with a linearised model

If iron saturation, flux crosscoupling and eddy-current damping are ignored, the DC machine can be represented by a set of analytic, but nonlinear equations which, in normalised form, are

$$\begin{aligned}\dot{x}_1 &= a_{11}x_1 + b_{11}u_1 \\ \dot{x}_2 &= a_{21}x_2 + a_{22}x_1x_3 + b_{22}u_2 \\ \dot{x}_3 &= a_{31}(x_1x_2 - T_L)\end{aligned}\quad (1)$$

where

$$a_{11} = \frac{1}{T_f}, \quad a_{21} = \frac{1}{T_a}, \quad a_{22} = -b_{22} = -\frac{1}{L_a}$$

$$a_{31} = \frac{1}{2H}, \quad b_{11} = \frac{1}{L_f}$$

and

$x_1$ = field current	$u_1$ = field voltage
$x_2$ = armature current	$u_2$ = armature voltage
$x_3$ = speed	$T_L$ = load torque
$L_f$ = field inductance	$T_f$ = field time constant
$L_a$ = armature inductance	$T_a$ = armature time constant
$H$ = inertia constant	

If the field is considered to be constant, these equations simplify to a linear, second-order model as follows:

$$\begin{bmatrix} \dot{x}_2 \\ \dot{x}_3 \end{bmatrix} = \begin{bmatrix} a_{21} & a_{22} \\ a_{31} & 0 \end{bmatrix} \begin{bmatrix} x_2 \\ x_3 \end{bmatrix} + \begin{bmatrix} b_{22} & 0 \\ 0 & 0 \end{bmatrix} \begin{bmatrix} u_2 \\ 0 \end{bmatrix}\quad (2)$$

For a particular medium-sized steel mill drive

$$\begin{aligned}a_{11} &= -1.0, & a_{21} &= -6.67, & a_{22} &= -133.3 \\ a_{31} &= 2.77, & b_{11} &= 1.0, & b_{22} &= 133.3\end{aligned}$$

Paper 3114B (P1), first received 11th July 1983 and in revised form 20th February 1984

Dr. Cardwell is with Marconi Space & Defence Systems Ltd., Frimley, Camberley, Surrey GU16 5PE, England and Dr. Goodman is with the Department of Electronic & Electrical Engineering, University of Birmingham, Birmingham B15 2TT, England

In this linearised case  $x_1$  is set to 1.0 p.u., and a performance index used as follows:

$$J = \int_0^T \left( x^T \begin{bmatrix} \lambda_3 & 0 \\ 0 & \lambda_0 \end{bmatrix} x + u^T \begin{bmatrix} \lambda_2 & 0 \\ 0 & 0 \end{bmatrix} u \right) dt \quad (3)$$

where

- $\lambda_0$  = speed weighting
- $\lambda_2$  = armature-voltage weighting
- $\lambda_3$  = armature-current weighting

By arbitrarily setting  $\lambda_2 = 1$ , the optimal pole positions become a function of  $\lambda_3$  and  $\lambda_0$ , and the values can be found using a frequency domain analysis [4]. It is found that a stable solution exists for positive  $\lambda_3$  and  $\lambda_0$ , and the condition for overdamping is  $\lambda_3 > 0.0390 + 0.0416 (1 + \lambda_0)^{1/2}$ . Fig. 1 shows the results for the particular case of

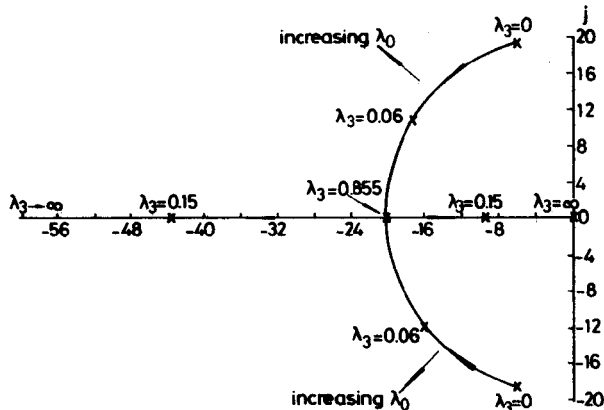


Fig. 1 Root locus plot of fixed field linear model

$\lambda_0 = 0.25$   
 $\lambda_2 = 1.0$

$\lambda_0 = 0.25$  where it can be seen clearly how  $\lambda_3$  increases the damping. It will be seen later that these results are in close agreement with the results obtained from the nonlinear system model when little field control is used; i.e. principally below base speed. This use of an algebraic optimisation procedure for a simplified linear model is thus valuable in giving guidance for the choice of error weighting factors which can be easily related to classical control concepts.

## 2.2 Time domain approach with a nonlinear model

Pontryagin's method may be applied directly to the nonlinear model (eqn. 1), resulting in a two-point boundary value problem. The Pontryagin optimal trajectories were obtained digitally by the direct sensitivity method [5], often requiring several iterations to solve the two-point boundary-value problem. The technique may include constraints on armature voltages and current although this often leads to convergence difficulties requiring accurate estimation of the adjoint variable initial conditions. Software refinements were incorporated to aid integration in the presence of state-variable limits and initial-condition estimation. Fig. 2 is an example of how the optimal control is influenced by an armature current limit (1.1 p.u.).

The performance index was

$$J = \int_0^T (\lambda_1 x_1^2 + \lambda_3 x_2^2 + \lambda_0 x_3^2 + \lambda_1 u_1^2 + \lambda_2 u_2^2) dt \quad (4)$$

The choice of weighting coefficients was based on the frequency-domain solutions for the fixed-field model, and adjusting the field-current weighting  $\lambda$  and field-voltage weighting  $\lambda_1$  by trial and error. The response to a step-

speed demand has been used primarily as the basis for performance evaluation. The speed response corresponded

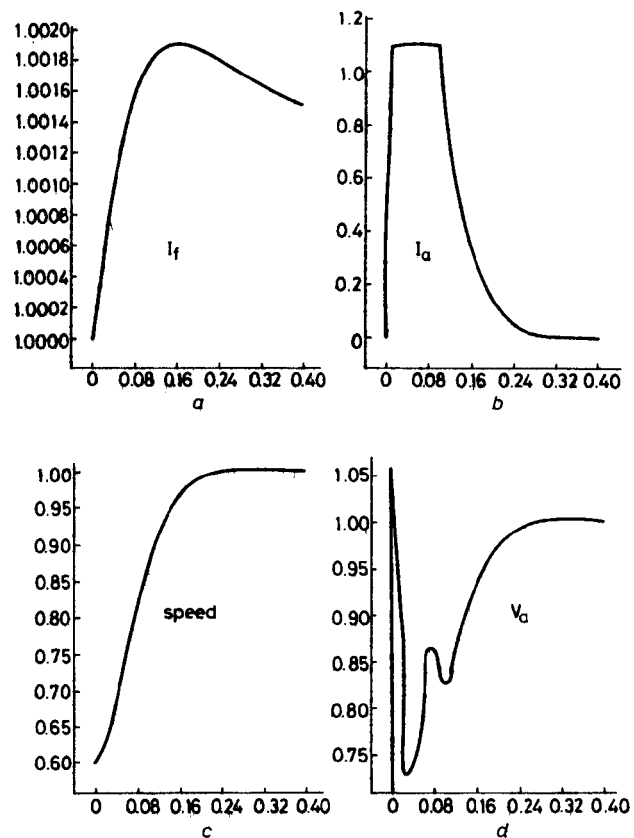


Fig. 2 Nonlinear model, optimal response with armature current saturation

a Trajectory of  $x_1$  against time  
b Trajectory of  $x_2$  against time  
c Trajectory of  $x_3$  against time

d Trajectory of  $u_2$  against time  
 $\lambda = 1.000, \lambda_0 = 0.250, \lambda_1 = 1.000$   
 $\lambda_2 = 1.000, \lambda_3 = 0.0600$

closely to the predictions of frequency domain analysis. With  $\lambda_0$  set at 0.25 and  $\lambda_2$  at 1.0, varying the armature-current weighting controlled the system damping similarly to the root locus plot of Fig. 1. The weighting on armature voltage was reduced from 1.0 to 0.01 to permit a greater transient variation in the control. This is equivalent to increasing loop gain. By experimenting with  $\lambda_3$  a value of 0.0005 was found to give a fast optimal speed response with little overshoot. This was the best speed trajectory established by means of the direct-sensitivity method. Further reduction of  $\lambda_2$  only caused  $\mu_2$  to limit and increased convergence difficulties.

So far only the step response with negligible field control has been considered. For larger speed steps above base speed, it is necessary to weaken the field to maintain control and speed of response. This field weakening above a nominal base speed is introduced into the optimal controls by changing the steady-state value of the field current over the optimisation period. The weighting on the field current was doubled to increase the field-weakening effect during the control, and  $\lambda_1$  was reduced to 0.01 to permit greater field forcing to quicken the field-current response. In Fig. 3 the field-weakening range chosen was in accordance with that required by the conventional system described in Section 3, for direct comparison in performance.

The virtue of these trajectories is that they maintain the same response as that achieved below base speed. However, this is obtained by using considerable armature forcing initially, necessary to force up the armature current

quickly. Unfortunately, because of the extreme initial deviation of the armature voltage, it was not possible to obtain

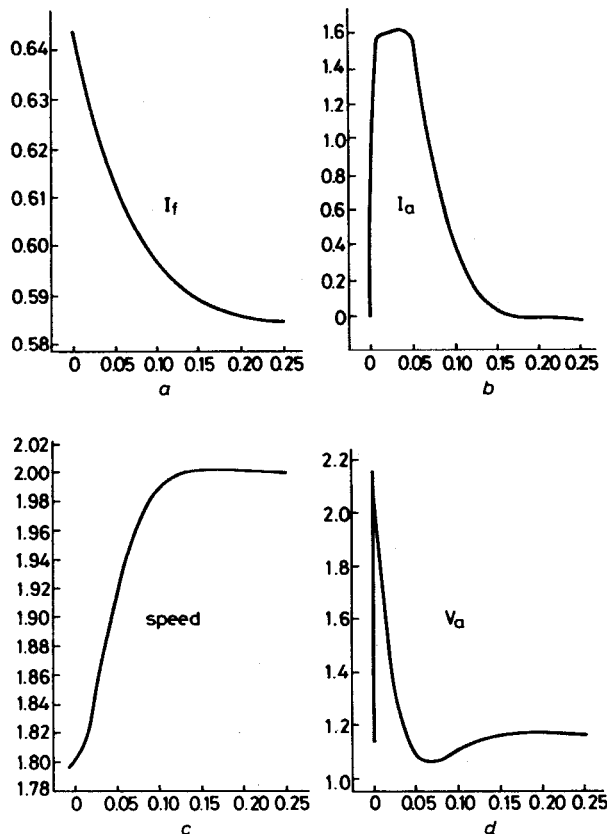


**Fig. 3** Nonlinear model, small step speed optimal response when field weakening

a Trajectory of  $x_1$  against time  
b Trajectory of  $x_2$  against time  
c Trajectory of  $x_3$  against time

d Trajectory of  $u_2$  against time  
 $\lambda = 2.000, \lambda_0 = 0.250, \lambda_1 = 0.010$   
 $\lambda_2 = 0.010, \lambda_3 = 0.0005$

convergence when a constraint of 1.2 p.u. was placed on  $u_2$ . Increasing the weighting on armature voltage is one possible way of preventing excessive armature forcing, but this would undoubtedly slow down the speed response. From the results presented here, the optimal controls are clearly formed in a manner which maximises the product of armature and field current while the speed error is large, in order to reduce the speed error quickly. The precise interaction of state and control variables that is used to maximise torque over most of the trajectory depends on the weighting coefficients.

### 3 Conventional spillover field-weakening controller

Having established various optimal solutions, it is necessary to compare these trajectories with the response of a conventional speed-control system for the same machine. Such a feedback controller is designed by classical frequency-domain methods. The behaviour of the complete speed controller is quite nonlinear, and good classical design of the individual loops is no guarantee of a well designed system. However, because the main system time constants are reasonably well spaced, it is possible to start by considering each loop separately.

#### 3.1 Design and stabilisation of the conventional controller

All four loops were designed to achieve a steady-state error of 1% or better, the response being tailored by transitional lag compensators of the form  $(1 + sT_1)/(1 + sT_2)$  in the

forward path. For the spillover loop, a logical choice for the compensator lead-time constant is to 'cancel' the field-current controller closed-loop time constant; in this example 0.01 s. The compensator lag time constant was chosen by simulation tests and was found to need a minimum value of 0.25 s of stable operation of the spillover loop. Unfortunately, this introduces an appreciable delay into the operation of the spillover control and any further increase in the compensator lag only makes this effect worse.

#### 3.2 Performance predicted by digital simulation

First, the digital simulation was run for a 4% change in speed demand just below the field-weakening region. Operating in this manner the speed response was slightly less than critically damped, with 10% overshoot. The trajectories were compatible with that expected of a well designed linear speed-control loop.

By performing a small step speed change in the field-weakening region (Fig. 4), a less damped response resulted. Evidently this is the cost of rapid field variation, caused by transients taking the armature voltage  $u_2$  above 1 p.u. Another feature of the spillover controller, observed on the simulation, was the delay in the spillover loop which occurs when entering the field-weakening region. This delay causes the field current to be at its full-field level for up to 0.3 s after the speed goes above 1 p.u.

#### 3.3 Comparisons with optimal solutions

The results of the simulation show several interesting features of operating in the spillover region:

- (i) less well damped speed response
- (ii) underdamped nature of the spillover control loop
- (iii) influence of the constraints on armature-voltage and armature-current reference

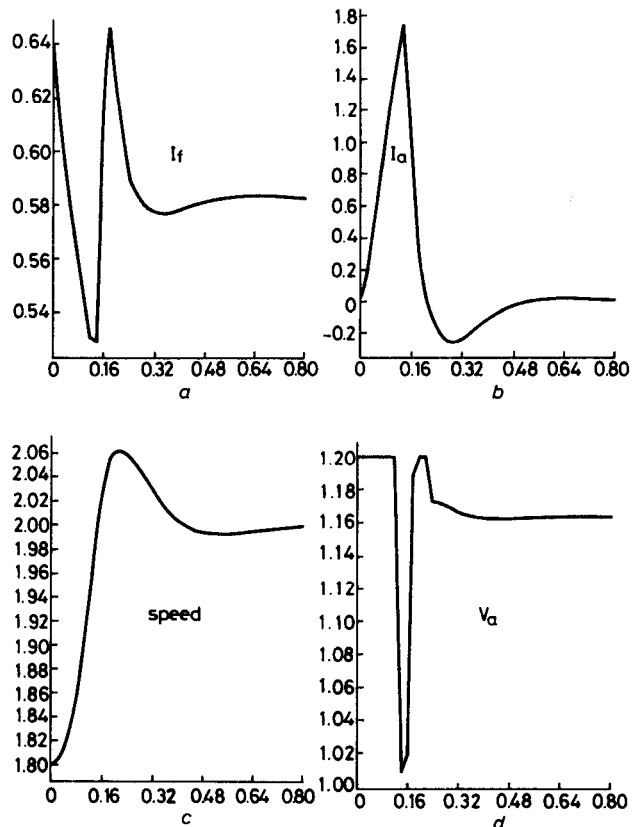


**Fig. 4** Spillover system, small step speed response when field weakening

Trajectories for a spillover field weakening drive

a Trajectory of  $x_1$  against time  
b Trajectory of  $x_2$  against time

c Trajectory of  $x_3$  against time  
d Trajectory of  $u_2$  against time

(iv) field-weakening delay on entry into the spillover region.

These peculiarities cause most operators of spillover controllers to insert a ramp-referencing circuit to avoid the possibility of a large step demand.

#### 4 Development of a near-optimal controller

Recognising that a direct synthesis of optimal nonlinear systems is not feasible, attention was turned to designing a feedback field controller which would come close to optimal. To eliminate the spillover delay a new field-weakening loop is required which does not depend on armature voltage for its driving signal. The overriding problem with the spillover drive is the constrained armature voltage, preventing rapid field-weakening on large-step transients. An alternative way of setting the required field level is by using the speed reference. The desired field current in steady state is determined from a field-current control law. The speed error is used for transient field control, thus retaining the information implicit in the speed feedback signal itself. In this way the field-weakening loop gain is recovered transiently.

The starting point of the design was to find the small-signal transfer function between the speed error and field current, which constitutes the feedback-path of the new controller. This proved to be proportional to armature current. The feed-forward compensation required to give a desirable open-loop response was a current-adjusted gain, inversely proportional to armature current, and a transitional lag compensator to shape the form of the transient response (Fig. 5). Another feature of this transient field adjustment (TFA) is the inhibiting of field-weakening until the speed has reached base speed. This prevents the motor accelerating on reduced torque unnecessarily for speed changes from below base speed.

##### 4.1 Simulation of TFA Controller

A digital simulation was developed to determine suitable values of TFA loop gain  $k$ , and the compensator lag time constant  $T_{TFA2}$ . The lead time constant was set to cancel the small-signal field-current controller time constant, as was the case for the spillover loop compensator. Because the TFA controller has the same speed and field current

control loops as the conventional drive, the digital simulation is similar to that of the spillover system, excepting the field demand configuration. A complication to the simulation exists when implementing the current-adjusted gain, because, as the armature current goes to zero, the loop gain becomes infinite. This is obviously unacceptable, not only in the simulation, but also on a real drive. The solution was to use a constant gain characteristic at low armature currents.

The determination of the best values for the parameters  $k$  and  $T_{TFA2}$  was by trial and error using the simulation. Since for practical values of  $k$  the TFA steady-state loop gain is small, large variations in the parameter values do not affect stability. Basically the time constant sets the speed of the field response, and the gain modifies the shape of that response. The parameter values which were found to give the most desirable performance over a wide range of demands were  $k = 0.05$  and  $T_{TFA2} = 0.075$  s.

##### 4.2 Comparison with spillover controller

Since the spillover and TFA controllers use the same speed loop, the performance below base speed is identical. For this reason the results presented here concentrate on operation in the field-weakening region.

For small speed demand steps just above base speed, the two controllers achieve very similar speed responses although it is worth noting that the delay in reducing the field current, which is characteristic of the spillover system, is eliminated in the TFA system. Nevertheless, since most of the control is achieved via the armature, the effect on the speed response is negligible. Further into the field-weakening range, the responses of the two controllers exhibit differences principally in the behaviour of the field current. As can be seen in Fig. 6, the field-current reduction is much closer to the optimal trajectory than is the poorly damped response shown in the spillover case. This results in a slight reduction in the speed overshoot and an improvement in the speed response, measured in integral of speed error-squared terms, of some 10%.

These results show, as expected, that the TFA controller has advantages for transients occurring above base speed. This effect is even more pronounced for large step changes. For example, using the same measure of speed-response performance, a reduction of 34% is achieved by the TFA

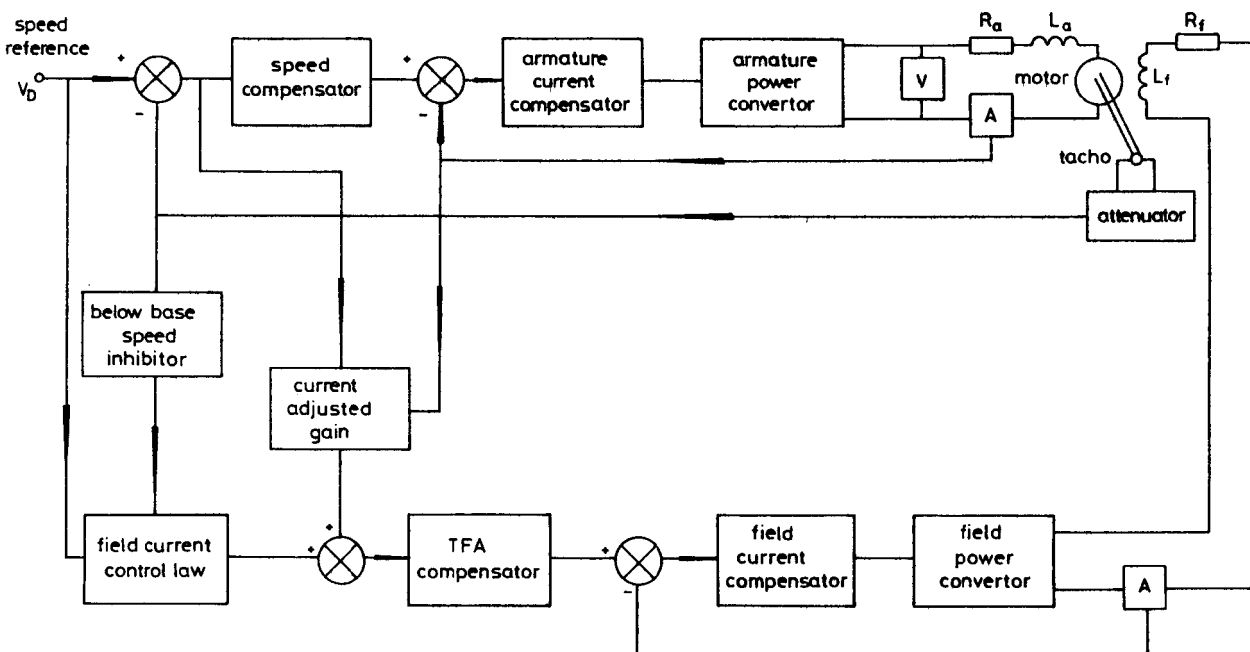


Fig. 5 Block diagram of the transient field adjustment controller

controller when the demand goes from 1.0 p.u. to 2.0 p.u. speed. Fig. 11, giving trajectories from actual drives to be

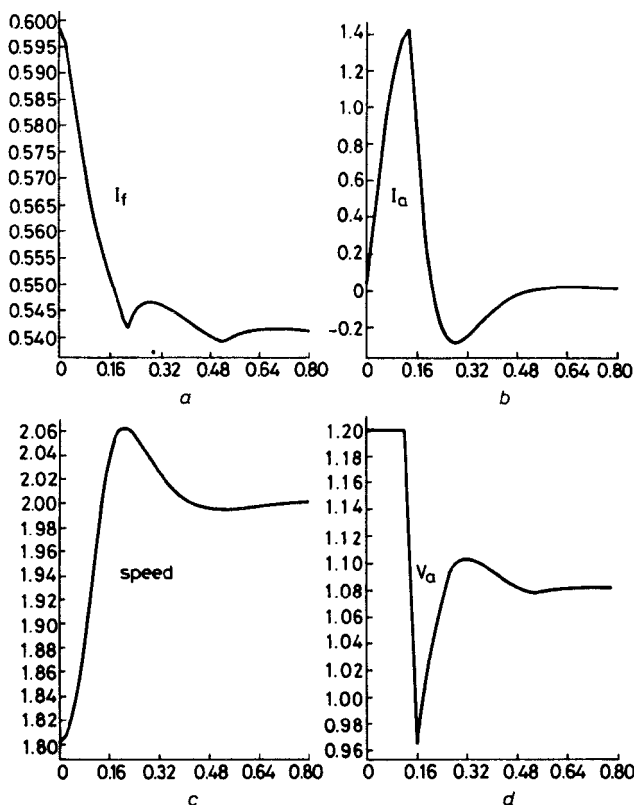


Fig. 6 TFA System, small step speed response when field weakening

Trajectories for a transient field adjustment drive  
a Trajectory of  $x_1$  against time      b Trajectory of  $x_2$  against time  
c Trajectory of  $x_3$  against time      d Trajectory of  $u_2$  against time

described later, shows responses for a 0–1.667 p.u. step where the difference in the field behaviour can be clearly seen, as can the consequent effect on the speed response itself.

## 5 Laboratory implementation of industrial speed controller

As a result of the digital simulations, the TFA system appeared to have sufficient advantage to justify the construction of a small reversible variable-speed laboratory drive to test the scheme under simulated industrial conditions.

### 5.1 Determination of machine parameters

Before considering the design of the speed control loop, a set of equations which accurately described the laboratory machine had to be determined. The most suitable machine available was a 5 horsepower, 200 V DC series machine with interpoles, which was operated as a separately excited motor to permit several times field forcing.

The set of base values for the motor were as follows:

1 p.u. voltage	= 220 V
1 p.u. current	= 17.35 A
1 p.u. resistance	= 12.68 $\Omega$
1 p.u. speed	= 1200 revs./min
1 p.u. torque	= 29.64 Nm
1 p.u. time	= 1 s
1 p.u. power	= 5 horsepower = 3.73 kW

The rated machine values in per unit terms were as follows:

rated armature voltage	= 1 p.u.
rated armature current	= 1 p.u.

rated speed	= 1 p.u.
rated field voltage	= 0.0358 p.u.
rated field current	= 1.406 p.u.
rated power	= 1 p.u.

These values were chosen to prevent two base systems for voltage and current being introduced. When the established parameters were substituted into the nonlinear p.u. machine equations, the basic machine equation set which resulted was

$$\left. \begin{aligned} \dot{x}_1 &= 6.67x_1 + 261.6u_1 \\ \dot{x}_2 &= -105x_2 - 448.9x_1x_3 + 631.1u_2 \\ \dot{x}_3 &= 0.508x_1x_2 - 0.714T_L \end{aligned} \right\} \quad (5)$$

### 5.2 Design of spillover and transient field adjustment loops

The field-weakening loops were designed to give a maximum speed of twice base speed. The complete spillover controller in block diagram form is given in Fig. 7. It was found necessary to adjust the lag term in the spillover compensator not only for stability reasons, but also to prevent excessive armature converter ripple from reaching the field-current controller. However, the time constant was still kept as short as possible to minimise spillover delay.

The design of the TFA loop was similar to the earlier example, with two modifications to take into account the reversibility of the laboratory drive. This was to ensure that when reversing the drive the controller never operated unnecessarily on weak fields. The modified TFA control loop of Fig. 8 includes values of the  $k$  and  $T_{TFA2}$  parameters which were chosen experimentally. A rigorous analysis of the TFA loop was not a prerequisite to determine  $k$  and  $T_{TFA2}$ , which were more easily determined by trial and error, either using simulation or on the drive itself.

Analogue hardware was used to build the drive, including two analogue multipliers in the TFA loop. A diode shaping circuit implemented the hyperbolic field-weakening control law, while the other functions were built around comparators and operational amplifiers.

### 5.3 Laboratory comparison of spillover and TFA controllers

Both laboratory controllers were examined under steady-state and transient operations.

#### (i) Steady state operation

The difference in the principle of operation of the two controllers is exemplified by the field-weakening control laws. The hyperbolic field-weakening law keeps the armature voltage at 1.0 p.u. for all speeds, increasing above this value when loaded, whereas the spillover control law increases the armature voltage above base speed by an amount determined by the spillover voltage range. However, the regulatory nature of the spillover controller ensures only a small increase in armature voltage on load. Although a 10% spillover range is used here, some modern drives use a 2–5% spillover range with better voltage regulation under load.

The speed regulation of both controllers on load was identical (see Fig. 9), and better than 1% at full field. This is evidence that the regulation of both controllers depends on speed loop gain, rather than field control. The field current of the TFA drive was constant on load, the armature voltage changing to accommodate the extra  $I_a R_a$  voltage drop. No problem was encountered with excessive

terminal voltage on load. Should this occur the field-weakening regime could be started just below base speed

tested for large signal response by measuring the 'top-to-top' reversal time, (i.e. the time to go from 2 p.u. forward

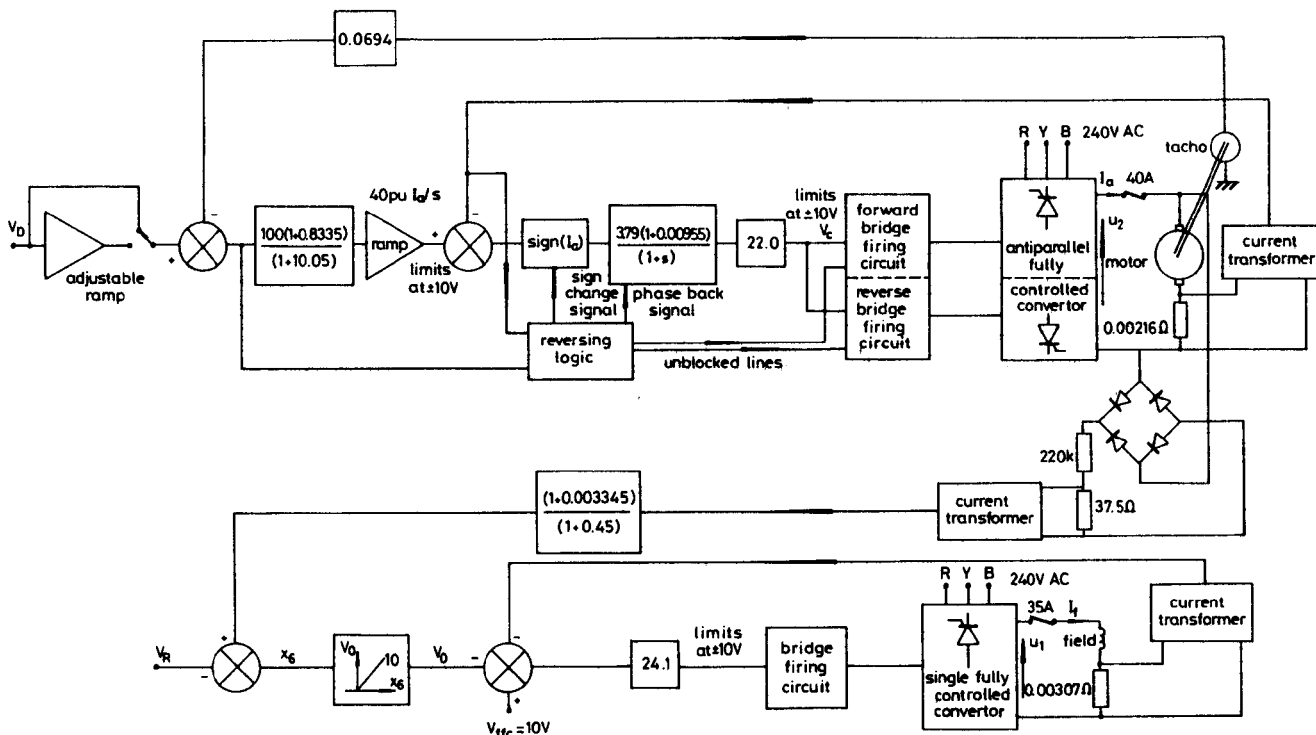


Fig. 7 Block diagram of laboratory spillover drive

to keep the steady-state terminal voltage within permitted bounds.

(ii) Transient operation

The small step speed responses for both controllers appear identical despite the elimination of spillover delay (see Fig. 10). This is primarily because of the predominant armature current control which overrides field changes for small step speed demands. All the measured transient responses presented here were confirmed by digital simulation of both controllers.

When larger transients are considered, the differences become more apparent. For example, the drives were

speed to 2 p.u. reverse speed). This is a fairly demanding test for the field control since it involves first strengthening the field from weak field to full field and then reducing it back to weak field again. The spillover drive took about 5 s to achieve the reversal, whereas the TFA drive took about 3.5 s, the difference being partly due to delay in starting to strengthen the field, partly due to delay in weakening the field which resulted in armature voltage limiting and consequent loss of torque, and partly due to the poorly damped nature of the spillover loop contributing to a speed overshoot.

Many manufacturers include a speed demand rate-limiting circuit (or speed reference ramp) in order to

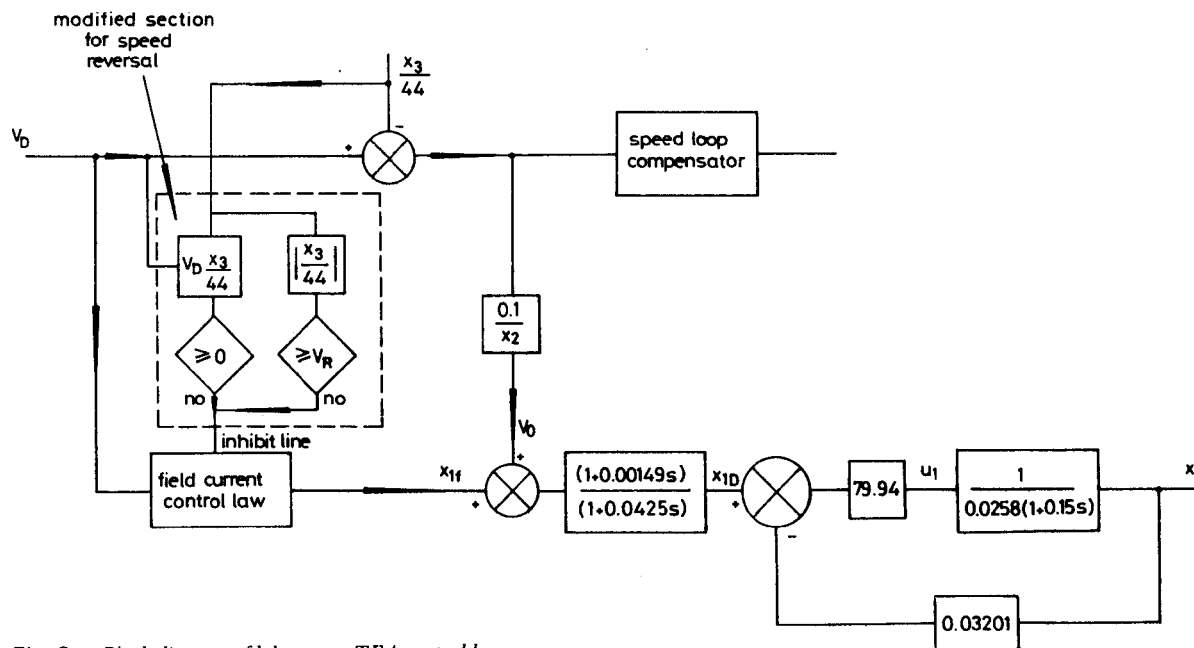


Fig. 8 Block diagram of laboratory TFA control loop

prevent step demands being applied directly to the speed controller. This is done essentially to prevent the sort of behaviour shown by the spillover drive in Fig. 11, where a comparison is made between the two control schemes

responding to a 0–1.667 p.u. speed step demand. An adjustable ramp circuit was included in the laboratory drives which was initially set at the fastest rate which just prevented armature voltage limiting in the TFA drive. The

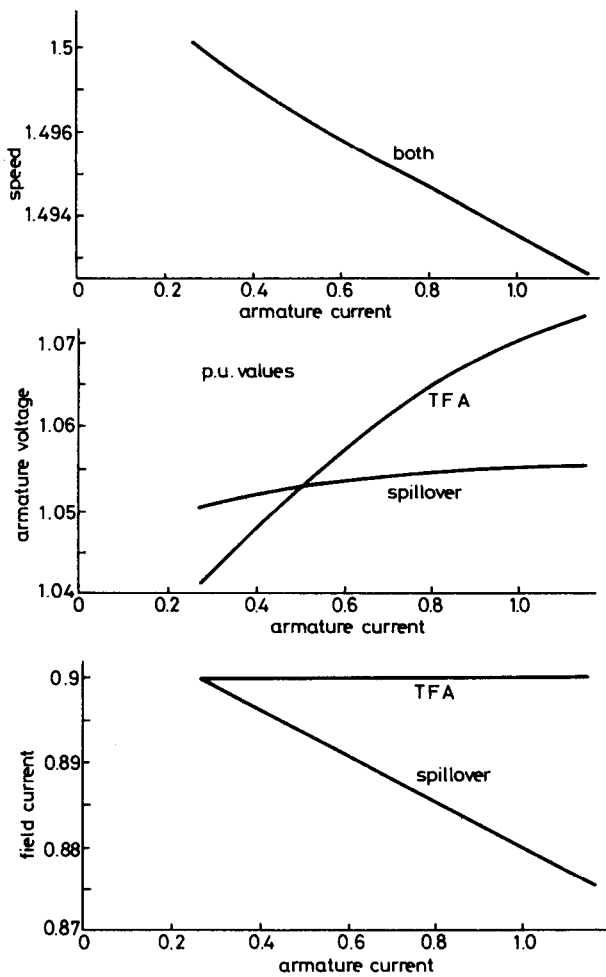


Fig. 9 TFA and spillover drives, load regulation comparison

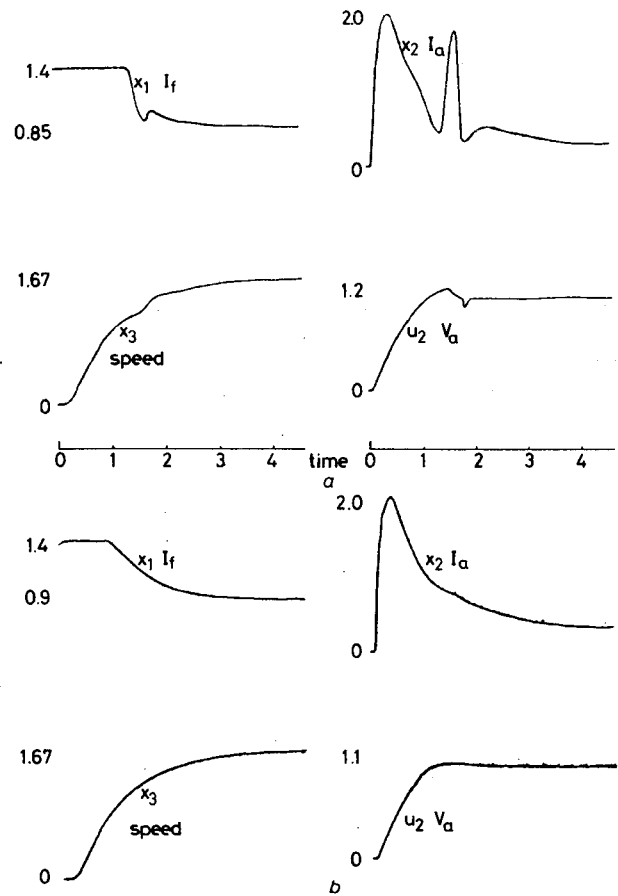


Fig. 11 Laboratory comparison, 0–1.67 p.u. speed change with a fast ramp input

a Trajectories of spillover drive  
b Trajectories of TFA drive

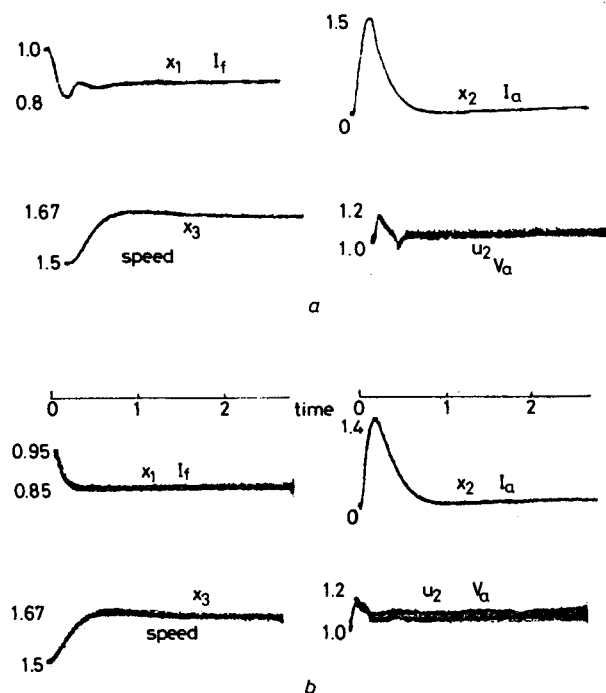


Fig. 10 Laboratory comparison, small step 1.5–1.67 p.u. speed

a Trajectories of spillover drive  
b Trajectories of TFA drive

results in Fig. 11 are for this setting; it can be seen quite clearly that the corresponding response for the spillover drive involves a period of armature-voltage limiting and a consequent loss of torque. Experiments conducted for other magnitudes of step inputs confirmed that this ramp setting was the best for the TFA drive for all conditions.

Despite the obvious differences in the configuration of the two controllers, their behaviour is for the most part very similar, with the important exception of transients requiring rapid field changes. An interesting demonstration of this fact was obtained by continuing to decrease the ramp rate setting until the spillover drive was also prevented from reaching armature-voltage limit. This required a considerably slower ramp setting, but the responses from both drives were then almost identical; the results are shown in Fig. 12.

## 6 Conclusions

The main cause of suboptimal performance in a conventional controller is the poor dynamic behaviour of the spillover field-weakening loop. Its relatively high gain, poor stability and time delaying properties do not make it an ideal form of controller. Despite this it has been used universally in DC wide-range speed controllers for many years. The existence of these defects with the spillover system is acknowledged by drive designers to be a limiting

factor when setting the speed ramp rate. The principal advantage of the spillover system is its good armature

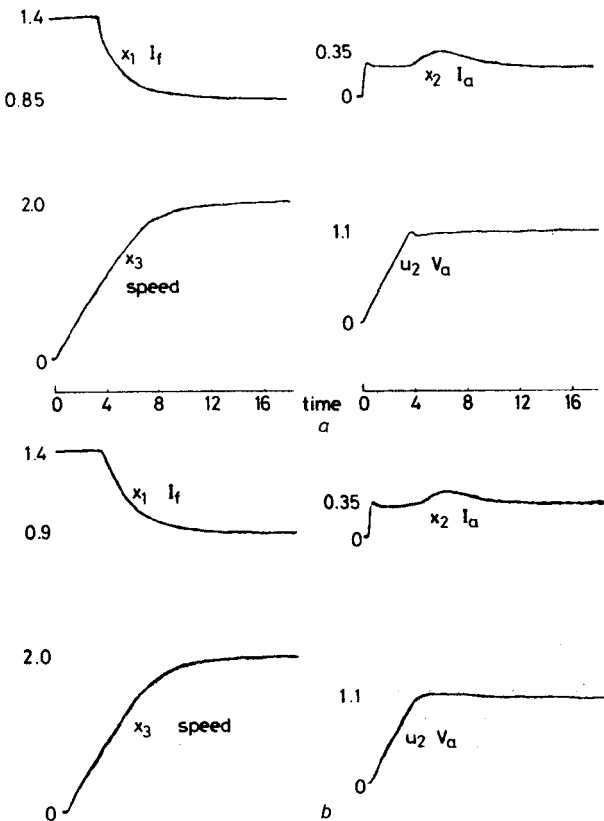


**Fig. 12** Laboratory comparison, 0–1.67 p.u. speed change with a slow ramp input  
 a Trajectories of spillover drive  
 b Trajectories of TFA drive

voltage regulation on load. Controllers have been manufactured with a spillover range of only 2%, which gives a very good voltage regulation, but at the expense of transient response.

The proposed TFA controller overcomes the stabilisation problem by behaving as an open-loop controller in steady state, being driven by a demand signal derived from the speed reference. The open-loop field response to a step input is a simple exponential, which is shaped by a transient adjustment signal derived from the speed error, so that the form of the speed response influences field weakening in a manner not dissimilar to the optimal control. This approach was adopted because of plant nonlinearities and constraints. The concepts behind the TFA

controller represent a compromise approach to the formulation of an ideal speed drive.

The basic advantage of the TFA controller is the elimination of field-weakening delay which makes it less likely to be subject to transient armature overvoltage. This was evident in the reduced armature-voltage and speed performance index terms. For example, a 22% reduction in the speed performance index term on a top-to-top speed change was achieved.

The TFA controller can operate with a faster ramp rate without over-voltage than its spillover counterpart. It is also easily set up because of the independent effects of gain and compensation, and the removal of the armature-voltage transducer and ripple. Noise from the tacho appeared on the speed error signal, but was not large enough to affect the transient adjustment signal.

Results from a laboratory implementation of the proposed drive confirmed the improved behaviour of the scheme in the upper speed ranges predicted by digital-computer simulation. The practical equipment inevitably included the details present in any real drive, e.g. tacho ripple, converter delay etc., and thus the direct application of the TFA proposal to existing drives has been shown to be possible, although some aspects of the drive behaviour, such as that under fault conditions, still need further investigation.

## 7 Acknowledgments

The authors would like to thank Prof. H.A. Prime and the University of Birmingham for the provision of laboratory and computing facilities, and engineers from GEC Electrical Projects Ltd., Rugby, for helpful discussions. One of the authors (B.J. Cardwell) would also like to thank the SERC for financial support received during the course of the work.

## 8 References

- 1 WHITE, B.A., LIPCZYNSKI, R.T., and DANIELS, A.R.: 'A simple digital control scheme for a DC motor', *IEE Proc. B, Electr. Power Appl.*, 1983, **130**, (2), pp. 143–147
- 2 PONTRYAGIN, L.S.: 'The theory of optimal processes' (Interscience Press, 1962)
- 3 BOR-RAMENSKII, A.E., and SUNG CHIEN: 'Optimum servo drive with two control parameters', *Autom. & Remote Control*, 1961, **22**, pp. 134–145
- 4 FALLSIDE, F., and SERAJI, H.: 'Design of optimal systems by a frequency domain technique', *Proc. IEE*, 1970, **117**, (10), pp. 2017–24
- 5 PAUL, R.J.A., and LEGGE, C.G.: 'Direct sensitivity method of solving boundary value problems in optimal control studies', *ibid.*, 1969, **116**, (2), pp. 273–280